

Applicability of point-dipoles approximation to all-dielectric metamaterials

A. Andryieuski,¹ S. M. Kuznetsova,² and A. V. Lavrinenko^{1,*}

¹*DTU Fotonik, Technical University of Denmark, DK-2800 Kongens Lyngby, Denmark*

²*Radiophysics Department, University of Nizhny Novgorod, Nizhny Novgorod 603950, Russia*

(Received 20 March 2015; revised manuscript received 10 June 2015; published 7 July 2015)

All-dielectric metamaterials consisting of high-dielectric inclusions in a low-dielectric matrix are considered as a low-loss alternative to resonant metal-based metamaterials. In this paper we investigate the applicability of the point electric and magnetic dipoles approximation to dielectric meta-atoms on the example of a dielectric ring metamaterial. Despite the large electrical size of high-dielectric meta-atoms, the dipole approximation allows for accurate prediction of the metamaterials properties for the rings with diameters up to ≈ 0.8 of the lattice constant. The results provide important guidelines for design and optimization of all-dielectric metamaterials.

DOI: [10.1103/PhysRevB.92.035114](https://doi.org/10.1103/PhysRevB.92.035114)

PACS number(s): 42.25.-p, 77.55.-g, 78.67.Pt

I. INTRODUCTION

In recent years metamaterials have aroused great attention as a tool for achieving desired electromagnetic properties, which might not exist in nature [1–5]. Among them a special attention has been paid to all-dielectric metamaterials [6–8], which are less restricted by dissipation losses compared to the metal-based ones. All-dielectric metamaterials with various constitutive units, such as spheres [9], cubes [10], and rods [11,12], were shown to exhibit negative magnetic permeability as well as negative [13–15] and zero refractive index [16]. Silicon nanodimers, exhibiting both electric and magnetic dipole responses, have recently been experimentally demonstrated to enhance electric and magnetic fields in the optical range [17]. High permittivity dielectric rings are of particular interest, because they possess a strong broadband magnetic response [18–20]. In addition, they have more degrees of freedom for tuning the resonance frequency by geometrical parameters than, for example, spheres, cubes or cylinders. Furthermore, they exhibit resonances on the THz frequencies [19–22], a very promising range for emerging applications. Appearing most frequently as periodical structures composed of subwavelength elements (the metamaterial lattice constant is on the order of $\lambda/20 - \lambda/4$), three-dimensional metamaterials are often treated as continuous media (the procedure referred to as *homogenization*) described by some effective parameters, e.g., permittivity ϵ , permeability μ , refractive index n , and impedance z , which simplifies their description. Various methods of homogenization have been suggested based on, for instance, field averaging, single-interface scattering, nonlocal dielectric function, and other approaches (see the brief overview of the methods in [23]). The most popular practical way of retrieving the effective parameters remains the Nicolson-Ross-Weir (NRW) or S-parameters method based on inversion of formulas for Fresnel's reflection and transmission coefficients. It was originally proposed for conventional media [24] and then extended to metamaterials [25]. The NRW method was accused of the loss of the retrieved effective parameters' physical meaning, since they do not satisfy the locality principle [26–29] and presence of the so-called “anti-resonance” [30] [nonphysical for pas-

sive materials $\text{Im}(\epsilon) < 0$ and $\text{Im}(\mu) < 0$; we assume optical exponential convention $\exp(-i\omega t)$]. Moreover, introduction of bulk effective parameters to metasurfaces or few layers metamaterials is questionable. Obviously the properties of a single layer or a layer with only few neighbors can be substantially different from the properties of a layer with many neighbors. In some cases of strong interaction between meta-atoms it is not possible to introduce any meaningful effective parameters [31].

We use another approach in which meta-atoms are replaced with point electric and magnetic dipoles [27,28,32–39]. The advantage of such an approach is that the interaction of dipoles can be explicitly taken into account either numerically for the arrays up to a few hundred by a few hundred elements or analytically for an infinite array [33].

Artificial magnetism of three-dimensional metamaterials composed of high-index dielectric spheres or cubes has been recently studied within the framework of modal analysis, NRW method, as well as single and dual dipole approximation [35–38]. It was concluded that the dual dipole approximation leads to rather accurate results. Nevertheless, the limitations of the applicability of the point-dipoles approximation to all-dielectric metamaterials are still a matter of dispute. In order to achieve strong resonant features, high refractive index dielectrics are typically used, and thus even geometrically sub-wavelength meta-atoms may become electrically (optically) larger than a wavelength exhibiting rapid field variations within their volume.

The goal of this work is to verify the applicability of the electric and magnetic dipole approximation for description of all-dielectric metamaterials. We make the study on the example of dielectric ring metamaterials. We start with considering a single layer of meta-atoms and investigate the dependence of their electric and magnetic polarizabilities of the geometrical parameters. Then in order to figure out the limits of the dipole approximation we show how the retrieved polarizabilities depend on the metamaterial lattice constant. Finally we consider a few layers of dielectric rings and compare the analytical predictions for reflectance R with the full-wave numerical simulations.

The paper is organized as follows. Section II is devoted to research methodology. The results of numerical simulation and its comparison with analytical prediction are presented in Sec. III. Discussion and conclusions are assembled in Sec. IV.

*alav@fotonik.dtu.dk

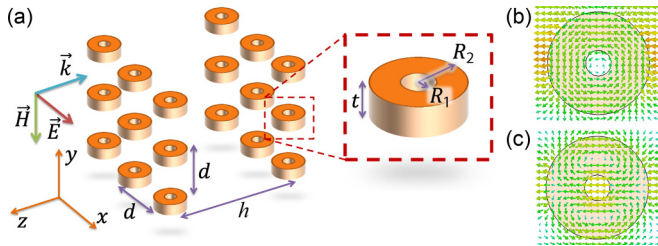


FIG. 1. (Color online) (a) Dielectric ring metamaterial consists of rings arranged in a square lattice. The plane wave is incident perpendicularly to the layers. Electric-field distribution in the unit cell for magnetic (b) and electric (c) dipole resonances that are excited with the incident plane wave.

II. METHODS

We consider dielectric rings of the outer and inner radii R_2 and R_1 , respectively, and thickness t arranged in the square lattice with lattice constant d within each layer and distance between the layers h [see the geometrical parameters in Fig. 1(a)]. The rings consist of dielectric with material permittivity $\varepsilon = 100 + i$ suspended in free space. A plane wave is normally incident along the z axis and its electric field directed along the x axis. We are interested in the lowest-order resonances of the rings classified as magnetic and electric dipole modes [see Figs. 1(b) and 1(c)].

In order to obtain electric and magnetic dipole polarizabilities $\tilde{\alpha}_e$ and $\tilde{\alpha}_m$ for an individual meta-atom, we treat every ring in the array as a combination of point electric and magnetic dipoles [32] oriented along the x and y axes, respectively, in correspondence with the polarization of the incident wave. The equivalent dipoles are positioned in the center of the rings. The electric \tilde{p} and magnetic \tilde{m} dipole moments are induced by the external field (amplitude of the electric and magnetic field are E_0 and H_0 , respectively and $E_0 = \eta_0 H_0$, where $\eta_0 = \sqrt{\mu_0/\varepsilon_0} = 120\pi[\Omega]$ is the free-space impedance) as well as by all the neighbors within the infinite array (interaction field $E_{\text{inter}}, H_{\text{inter}}$). In the case of a single layer, taking into account the identity of the dipoles, we express \tilde{p} and \tilde{m} :

$$\tilde{p} = \tilde{\alpha}_e(E_0 + E_{\text{inter}}) = \tilde{\alpha}_e(E_0 + \varepsilon_0 d^3 \beta^0 \tilde{p}), \quad (1)$$

$$\tilde{m} = \tilde{\alpha}_m(H_0 + H_{\text{inter}}) = \tilde{\alpha}_m(H_0 + \mu_0 d^3 \beta^0 \tilde{m}), \quad (2)$$

where the interaction constant β^0 is

$$\beta^0 = \text{Re} \left[\frac{ikd}{4} \left(1 + \frac{1}{ikR_0} \right) e^{ikR_0} \right] + i \left(\frac{kd}{2} - \frac{k^3 d^3}{6\pi} \right), \quad (3)$$

and $R_0 = d/1.438$ [33].

The amplitude reflection and transmission coefficients can be split into electric R_e and magnetic R_m terms [32]:

$$R = R_e + R_m, \quad T = 1 + R_e - R_m, \quad (4)$$

$$R_e = \frac{ikd}{2} \frac{1}{\frac{\varepsilon_0 d^3}{\tilde{\alpha}_e} - \beta^0}, \quad R_m = -\frac{ikd}{2} \frac{1}{\frac{\mu_0 d^3}{\tilde{\alpha}_m} - \beta^0}. \quad (5)$$

The polarizabilities of the particles are then expressed as

$$\tilde{\alpha}_e = \frac{\varepsilon_0 d^3}{\beta^0 + \frac{ikd}{2R_e}}, \quad \tilde{\alpha}_m = \frac{\mu_0 d^3}{\beta^0 - \frac{ikd}{2R_m}}. \quad (6)$$

We introduce the normalized dimensionless polarizabilities $\alpha_e = \tilde{\alpha}_e/\varepsilon_0 d^3$, $\alpha_m = \tilde{\alpha}_m/\mu_0 d^3$. Then the inverse polarizabilities are

$$\frac{1}{\alpha_e} = \beta^0 + \frac{ikd}{R + T - 1}, \quad \frac{1}{\alpha_m} = \beta^0 - \frac{ikd}{R - T + 1}. \quad (7)$$

Such an approach is computationally very efficient, since it requires simulations of a single unit cell with periodic boundary conditions (thus effectively an infinite two-dimensional array). It is applicable to meta-atoms with spectrally separated as well as overlapping electric and magnetic resonances such as, for example, in [40,41], as long as there is no magneto-electric coupling. Alternatively the electric and magnetic polarizabilities of an isolated particle can be retrieved with the surface integral equation method [34].

Considering two layers of particles one should take into account the interaction between the layers. The wave propagates as shown in Fig. 1(a), and the coordinate system origin is placed in the center of a ring in the first layer. The propagation occurs towards negative z , $E(z) = E_0 \exp(-ikz)$. The system of equations [33] for the normalized dimensionless dipole moments $p_{1,2} = \tilde{p}_{1,2}/(\varepsilon_0 d^3 E_0)$, $m_{1,2} = \tilde{m}_{1,2}/(\mu_0 d^3 H_0)$ reads

$$\frac{1}{\alpha_e} p_1 = 1 + \beta^0 p_1 + \beta^{-h} p_2 + \beta_{em}^{-h} m_2, \quad (8)$$

$$\frac{1}{\alpha_e} p_2 = \exp(ikh) + \beta^0 p_2 + \beta^h p_1 + \beta_{em}^h m_1, \quad (9)$$

$$\frac{1}{\alpha_m} m_1 = 1 + \beta^0 m_1 + \beta^{-h} m_2 + \beta_{me}^{-h} p_2, \quad (10)$$

$$\frac{1}{\alpha_m} m_2 = \exp(ikh) + \beta^0 m_2 + \beta^h m_1 + \beta_{me}^h p_1, \quad (11)$$

where the interaction coefficients can be found with approximate formulas (valid up to $kd \lesssim 1.5$) [33]

$$\begin{aligned} \beta^h &= -\text{Re} \left\{ \frac{-ikd}{4} \left[\left(1 + \frac{1}{ik\sqrt{R_0^2 + h^2}} \right) \right. \right. \\ &\quad \left. \left. + \frac{h^2}{R_0^2 + h^2} \left(1 - \frac{1}{ik\sqrt{R_0^2 + h^2}} \right) \right] e^{ik\sqrt{R_0^2 + h^2}} \right. \\ &\quad \left. + \frac{d^3}{4\pi} \left(\frac{1}{h^3} - \frac{ik}{h^2} - \frac{k^2}{h} \right) e^{ikh} \right\} + i \frac{kd}{2} \cos(kh), \\ \beta_{em}^h &= -i \frac{kd}{2} \frac{h}{\sqrt{R_0^2 + h^2}} e^{ik\sqrt{R_0^2 + h^2}}, \end{aligned} \quad (12)$$

and the following equalities are valid:

$$\beta^{-h} = \beta^h, \beta_{em}^h = -\beta_{me}^h = -\beta_{em}^{-h}. \quad (13)$$

Thus for two metalayers we get the system of linear equations for unknown dipole moments:

$$-\begin{bmatrix} \beta^0 - \frac{1}{\alpha_e} & \beta^h & 0 & \beta_{em}^h \\ \beta^h & \beta^0 - \frac{1}{\alpha_e} & -\beta_{em}^h & 0 \\ 0 & \beta_{em}^h & \beta^0 - \frac{1}{\alpha_m} & \beta^h \\ -\beta_{em}^h & 0 & \beta^h & \beta^0 - \frac{1}{\alpha_m} \end{bmatrix} \begin{bmatrix} p_1 \\ p_2 \\ m_1 \\ m_2 \end{bmatrix} = \begin{bmatrix} 1 \\ e^{ikh} \\ 1 \\ e^{ikh} \end{bmatrix}. \quad (14)$$

After finding the dipole moments one can calculate the electric and magnetic contributions to reflection and transmission coefficients:

$$R_e = \frac{1}{2}ikd(p_1 + p_2e^{ikh}), \quad (15)$$

$$R_m = -\frac{1}{2}ikd(m_1 + m_2e^{ikh}), \quad (16)$$

$$T_e = \frac{1}{2}ikd(p_1e^{ikh} + p_2), \quad (17)$$

$$T_m = \frac{1}{2}ikd(m_1e^{ikh} + m_2), \quad (18)$$

and finally obtain R and T :

$$R = \frac{1}{2}ikd(p_1 + p_2e^{ikh} - m_1 - m_2e^{ikh}), \quad (19)$$

$$T = e^{ikh} + \frac{1}{2}ikd(p_1e^{ikh} + p_2 + m_1e^{ikh} + m_2). \quad (20)$$

For larger number N of layers the procedure is analogical. At first one finds the dipole moments solving the system of equations

$$-\begin{bmatrix} \beta^0 - \frac{1}{\alpha_e} & \beta^h & \beta^{2h} & \vdots & \beta_{em}^{(N-1)h} \\ \beta^h & \beta^0 - \frac{1}{\alpha_e} & \beta^h & \vdots & \beta_{em}^{(N-2)h} \\ \beta^{2h} & \beta^h & \beta^0 - \frac{1}{\alpha_e} & \vdots & \beta_{em}^{(N-3)h} \\ \dots & \dots & \dots & \ddots & \dots \\ -\beta_{em}^{(N-2)h} & -\beta_{em}^{(N-3)h} & -\beta_{em}^{(N-4)h} & \vdots & \beta^h \\ -\beta_{em}^{(N-1)h} & -\beta_{em}^{(N-2)h} & -\beta_{em}^{(N-3)h} & \vdots & \beta^0 - \frac{1}{\alpha_m} \end{bmatrix} \cdot \begin{bmatrix} p_1 \\ p_2 \\ p_3 \\ \vdots \\ m_{N-1} \\ m_N \end{bmatrix} = \begin{bmatrix} 1 \\ e^{ikh} \\ e^{i2kh} \\ \vdots \\ e^{ikh(N-2)} \\ e^{ikh(N-1)} \end{bmatrix}, \quad (21)$$

and then calculates the reflection and transmission coefficients:

$$R = \frac{1}{2}ikd \sum_{n=1}^N (p_n - m_n)e^{ikh(n-1)}, \quad (22)$$

$$T = e^{ikh(N-1)} + \frac{1}{2}ikd \sum_{n=1}^N (p_n + m_n)e^{ikh(N-n)}. \quad (23)$$

We performed numerical full-wave simulations with CST Microwave Studio [42] in the time domain with effectively periodic (perfect electric along x and perfect magnetic along y axis) boundary conditions and normally incident plane-wave excitation.

III. RESULTS

For the rest of the paper we consider the thickness of the rings fixed to $t/d = 0.2$, distance between the centers of the rings in neighboring layers $h = d$, and variable inner and outer radii R_1, R_2 . The frequency range is $0-0.3 d/\lambda$ in order to stay within the metamaterial regime. To be noted, formulas (3) and (12) for the interaction coefficients are applicable for $kd \lesssim 1.5$ [33], which corresponds to $d/\lambda < 0.25$.

A. Variation of the outer R_2 and inner R_1 radii

In this section we investigate the influence of geometrical parameters, namely, the outer and inner radii on the resonant properties of the dielectric ring metamaterial. Let us fix the inner radius $R_1/d = 0.1$ and vary the outer radius in the range $R_2/d = 0.2-0.5$ (Fig. 2). The resonant peaks and dips are clearly seen in the reflectance spectra; for example, follow the blue line in Fig. 2(a). They correspond to the lower-order modes of the dielectric ring resonators, namely, the magnetic dipolar (lower frequency) and electric dipolar (higher frequency) modes. The corresponding electric-field distributions are shown in Figs. 1(b) and 1(c), respectively. Consequently, the retrieved electric [Fig. 2(b)] and magnetic [Fig. 2(c)] polarizabilities exhibit resonance behavior at the frequencies of the reflection maxima. Increase of the size of the rings expectedly leads to decrease in the resonant frequency and increase of the resonance strength [Figs. 2(b) and 2(c)]. Apart from the low-order dipolar modes some higher-order modes can be excited (see shaded area in Fig. 2); however, they are lying in the high-frequency zone and will be excluded from the further analysis.

When R_2 is fixed, but inner radius R_1 is varied, one of the reflection peaks stays almost unchanged whereas another one shifts dramatically [Fig. 3(a)]. Increasing R_1 influences strongly on the location of the electric dipole peak [Fig. 3(b)], but has weaker impact on the magnetic dipole [Fig. 3(c)]. The magnetic field of the excited resonance is induced by the circulation of the displacement current. According to the mode structure [Fig. 1(b)], it is obvious that the dominating contribution is given by the periphery of the ring. Overall the modes blueshift with the inner hole radius R_1 growth [Figs. 3(b) and 3(c)] as the result of the decreasing high-dielectric material filling fraction.

B. Applicability of the dipole approximation and variation of the array period

For retrieval of ring electric α_e and magnetic α_m polarizabilities, which are the characteristics of a single ring, we use formula (7) and simulate reflection and transmission for an infinite periodic array of the rings. The influence of the infinite number of neighbors is taken into account through interaction constant β^0 , for which accurate analytical formulas exist for the square array of point dipoles [33]. At the same time, the rings we consider here are not pointlike, but rather comparable

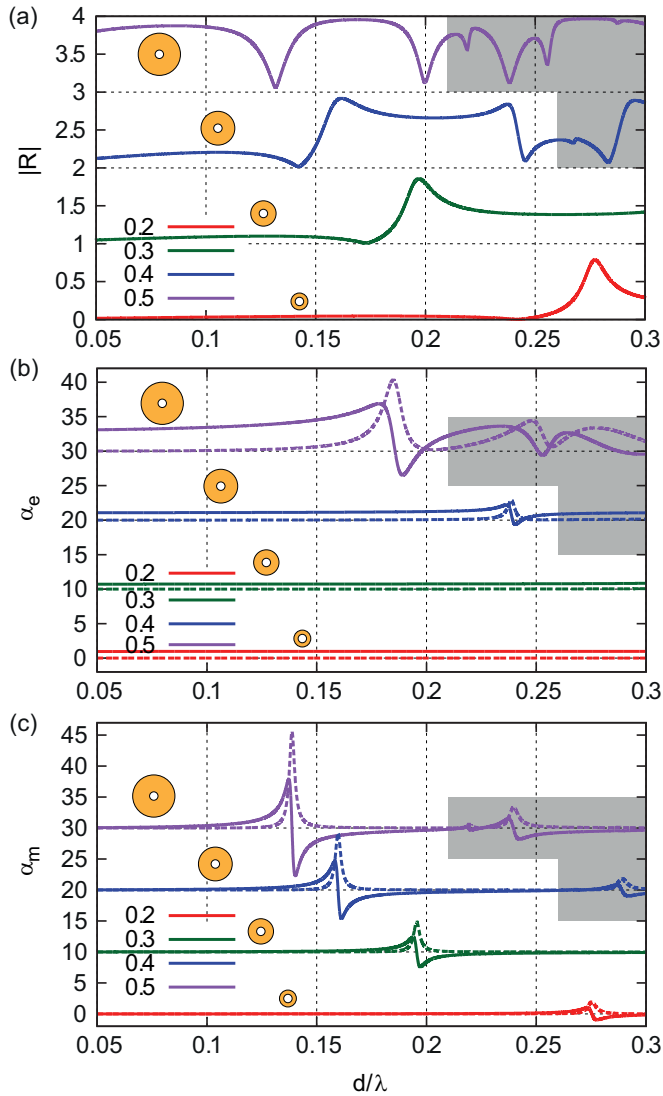


FIG. 2. (Color online) (a) Absolute value of the reflection R for a single array of rings, with dimensionless electric (b) and magnetic (c) polarizabilities. The inner radius is fixed to $R_1/d = 0.1$. The outer radius $R_2/d = 0.2$ (red), 0.3 (green), 0.4 (blue), and 0.5 (purple). For clarity of presentation a vertical incremental offset is introduced to the spectra. The offsets of the spectra are marked with horizontal dotted lines. This convention is kept throughout the rest of the paper. The gray-shaded areas mark the range where higher-order modes are excited.

to the period of the array. This may lead to both deviation of the field distribution of a certain dipole from the field of the dipole located in its center (thus, influence on polarizabilities α_e and α_m) as well as influence on the interaction field of all other dipoles (thus, influence on interaction constant β^0). We assume that interaction constant β^0 is the same as given by formula (7), and thus all effects related to the finite size of the rings are included into retrieved polarizabilities α_e and α_m . Then, retrieving the polarizabilities for the arrays of various periods we are able to characterize how different from the point dipoles the meta-atoms are (ideally the retrieved polarizabilities should not depend on the array period). We call the actual period of the structure d^* in order to differentiate it from the previously

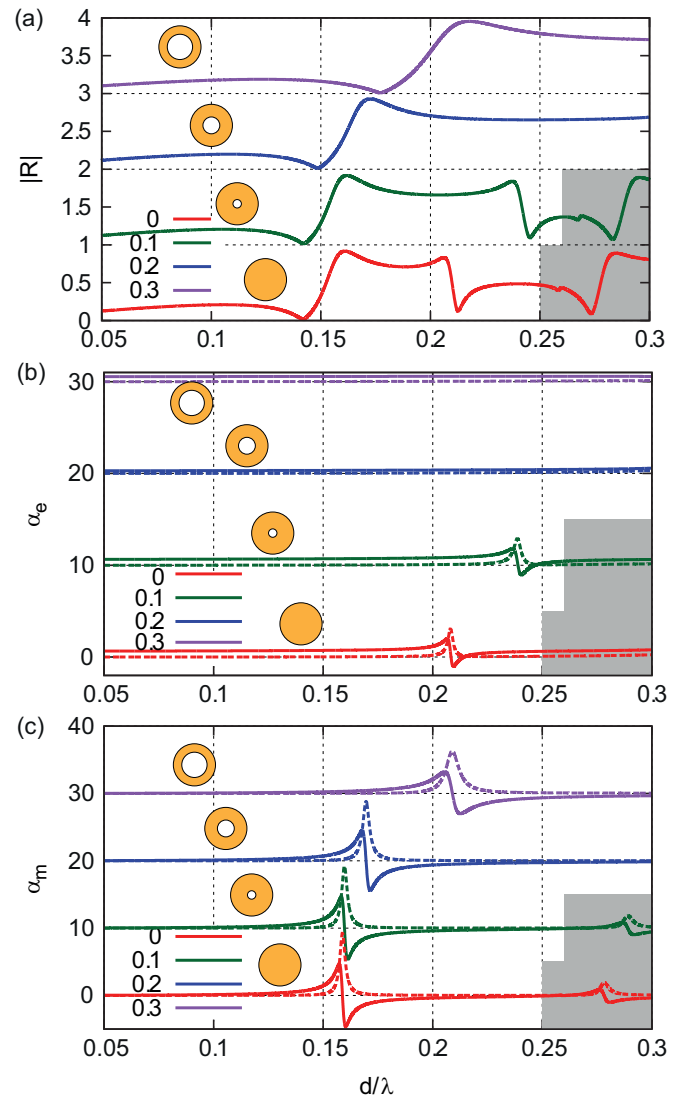


FIG. 3. (Color online) (a) Reflection R for a single array of rings and their dimensionless electric (b) and magnetic (c) polarizabilities. The outer radius is fixed $R_2/d = 0.4$. The inner radius varies, $R_1/d = 0$ (red), 0.1 (green), 0.2 (blue), and 0.3 (purple).

used constant d , while the latter is now used for normalization of frequency and polarizabilities only.

Period d^* influences the restored electric and magnetic polarizabilities (Fig. 4) and they converge to a certain value with increasing period d^* . Such behavior is natural, since the larger the period the smaller is the radius-to-period ratio R_2/d^* and, thus, the accuracy of the dipole approximation improves. Generally convergence of magnetic polarizabilities α_m [Figs. 4(a')–4(d')] is faster than electric α_e [Figs. 4(a)–4(d)], which can mean that magnetic interaction of the rings is weaker than electric. In case of touching rings ($d^* = 2R_2$) the retrieved polarizabilities differ much from the asymptotic value, clearly exhibiting failure of the point-dipoles approximation. Indeed, touching rings can hardly be considered as a set of separate rings, but rather as a periodic subwavelength grating or a perforated dielectric membrane. The polarizabilities convergence is good for the rings radii up to $R_2/d = 0.4$ [Figs. 4(a)–4(c) and 4(a')–4(c')]. For larger rings with $R_2/d = 0.5$ no convergence

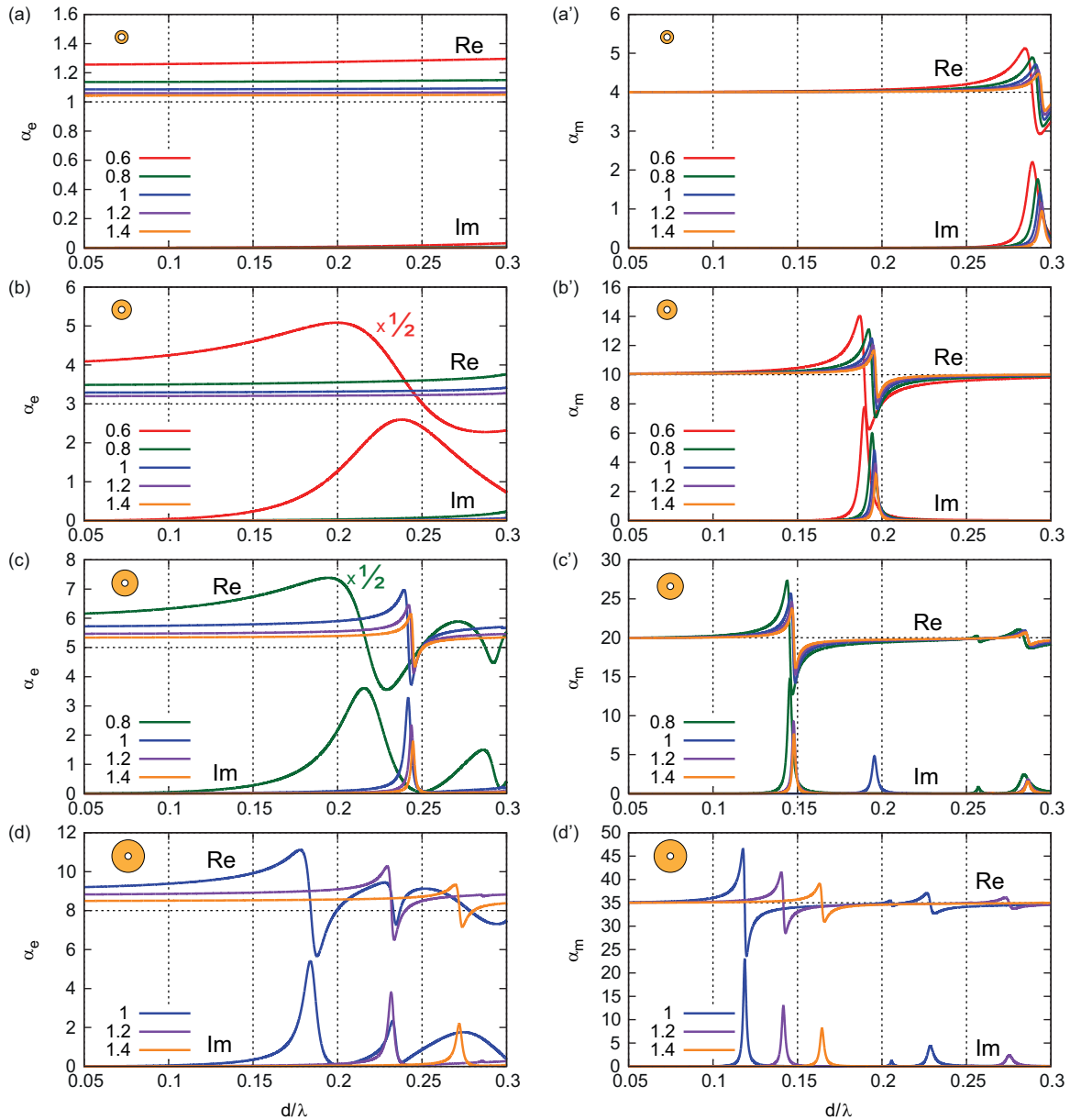


FIG. 4. (Color online) Normalized electric (a)–(d) and magnetic (a′)–(d′) polarizabilities for $R_2/d = 0.2, 0.3, 0.4,$ and $0.5,$ respectively. The values of the actual period d^*/d are (not on all graphs; only the cases of $d^* \geq 2R_2$ are shown) 0.6 (red), 0.8 (green), 1 (blue), 1.2 (purple), and 1.4 (orange). The real parts of the polarizabilities have positive offset for presentation clarity. The curves for $d^*/d = 0.6$ (red) in (b) and $d^*/d = 0.8$ (green) in (c) are multiplied by $1/2$ in order to fit the graph.

is observed for the period d^* up to $d^*/d = 1.4$ that lies on the boundary of the metamaterials regime and corresponds to $d^* \approx 0.5\lambda$ at the normalized frequency $d/\lambda = 0.3$ [Figs. 4(d) and 4(d′)]. Overall we may conclude that dipole approximation is consistent for the rings radius up to $R_2/d = 0.4$ and lattice constant $d^*/d > 0.8$.

C. Several layers structure

Knowing polarizabilities α_e and α_m of individual rings retrieved from the simulated reflection and transmission for a single layer, we may analytically predict the reflection and transmission for several layers of rings (see the methodology section for details). Direct comparison of these analytical

predictions to numerical simulations can give us additional evidences of applicability or nonapplicability of the point-dipoles approximation. We use the same rings geometrical parameters as in the previous subsection. Figure 5 shows the reflection for different R_2 for two, three, and four layers structure with $R_1/d = 0.1$ and $R_2/d = 0.2, 0.3, 0.4,$ and 0.5 .

For smaller radii $R_2/d = 0.2$ and 0.3 and even for $R_2/d = 0.4$ the analytical prediction is in a good correspondence with the numerical simulations, providing another confirmation that the dipole approximation works well [Figs. 5(a)–5(c)]. The discrepancy between the predicted and simulated results increases with R_2 and for the case of touching rings $R_2/d =$

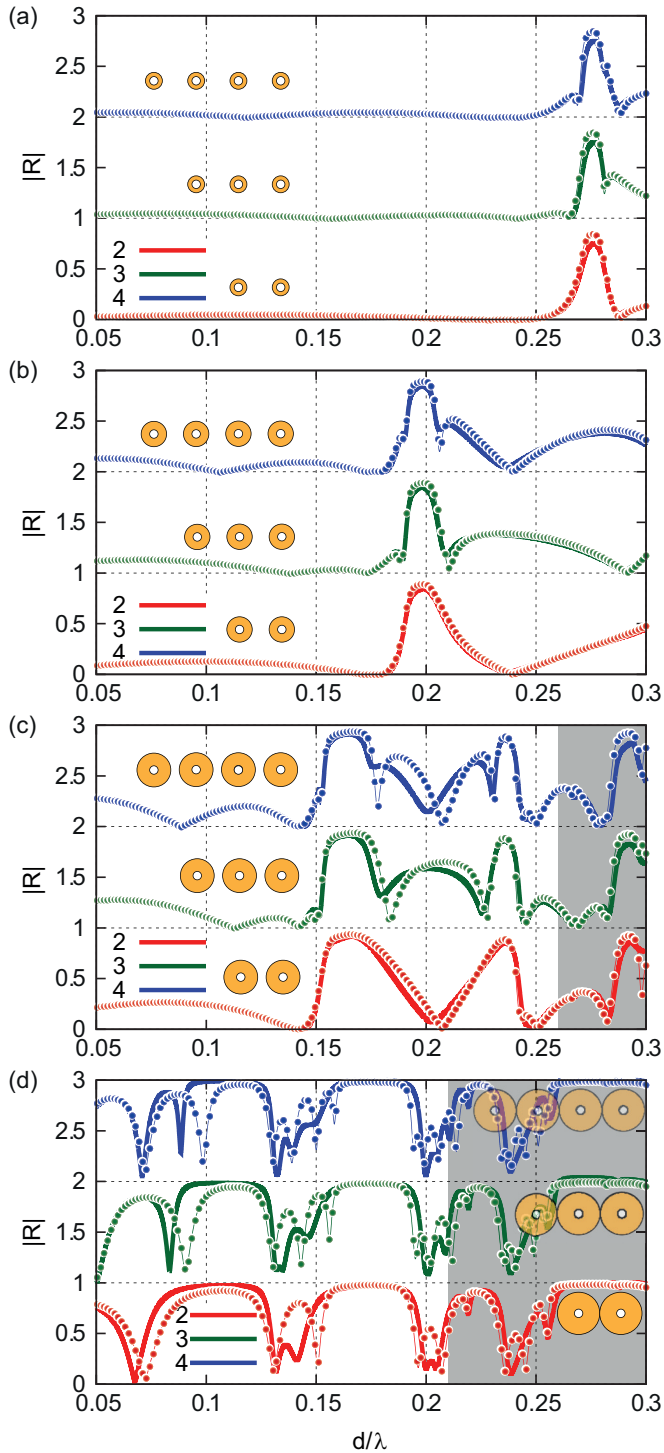


FIG. 5. (Color online) Absolute value of reflection $|R|$ for two (red), three (green), and four (blue) layers of rings. Analytical predictions (thick solid lines) are compared to full-wave numerical simulations (thin lines with circles). The inner radius is fixed, $R_1/d = 0.1$. The outer radius is $R_2/d = 0.2$ (a), 0.3 (b), 0.4 (c), and 0.5 (d). The gray area corresponds to the frequency range where high-order resonances are excited.

0.5 [Fig. 5(d)] the reflections given with two methods do not resemble each other reasonably, especially in the region of resonant peaks and dips. Interestingly, the reflection is different

not only in the region of polarizabilities resonances (see Fig. 2), but also in other regions of reflection dips, which we interpret as appearing due to Fabry-Perot resonances (increasing R_2 leads to the high-dielectric materials filling fraction increase and thus to the increase of the overall optical thickness of the metamaterial slab).

We may conclude that the electric and magnetic polarizabilities restored from a plane square-lattice array are able to predict the several layers reflectance for $R_2/d < 0.4$, but fail for larger radius.

IV. DISCUSSION AND CONCLUSIONS

We have analyzed electric and magnetic polarizabilities of the high-dielectric rings approximating them as point dipoles. The geometrical parameters and the free-space wavelength are normalized to the unit-cell size, thus the results of our analysis are wavelength independent and virtually are applicable to any frequency range.

Variations of geometrical parameters allow for tuning the resonance frequencies for α_e and α_m nearly independently: outer radius R_2 influences the resonance frequencies of both electric and magnetic polarizabilities (Fig. 2) while the inner radius predominantly influences electric polarizability α_e (Fig. 3).

We come to a natural conclusion that decreasing the structural unit size leads to a better prediction of the electromagnetic properties with the point-dipoles approximation. The dipole approximation works well for the rings up to $R_2/d = 0.4$ (Fig. 4). This value is surprisingly large, since the electrical size of the ring at the frequency $d/\lambda = 0.15$ is $2R_2n \approx 1.2\lambda$, thus the ring is not electrically small anymore and the field varies rapidly in space within the ring.

For larger rings the situation is different. The rings with the radius $R_2/d = 0.5$ are not isolated—they are literally touching each other. In this case the dipole approximation is not valid anymore. The retrieved polarizability changes dramatically with the lattice constant of the array [Figs. 4(d)–4(d')] and cannot predict the electromagnetic response for several layers [Fig. 5(d)]. Instead of isolated particles separated by the free-space gaps, we rather get a perforated high-index dielectric grating. Even though the period of the grating is smaller than the free-space wavelength, and thus no diffraction to the free space can happen, the guided mode in such dielectric membranes can be excited. The power coupled at some point is no longer localized within the particle, but can propagate within the dielectric layer, thus the metamaterial cannot be effectively homogenized.

We have investigated the metamaterial made of high-dielectric rings. Even though the selected $\epsilon = 100$ is modest (the dielectric constant of barium strontium titanate may reach several hundreds [43]), it is representative enough to make general enough conclusions. We may accurately anticipate the behavior of the lower-index dielectrics. They might be better suited to homogenization, having smaller refractive index contrast with the background. However, the unusual properties, based on strong electric and magnetic resonances, would also be weaker.

In conclusion, the all-dielectric ring metamaterials can be described with electric and magnetic point dipole approximation if the meta-atoms size (ring radius) is smaller than 0.8 of

the period. For the meta-atoms that almost touch each other, the dipole approximation is not applicable. We believe the presented methodology and analysis results will be useful for development of low-loss all-dielectric based metamaterials.

ACKNOWLEDGMENT

A.A. acknowledges financial support from the Danish Council for Independent Research via the GraTer project (Contract No. 0602-02135B).

-
- [1] M. A. Noginov and V. A. Podolskiy, *Tutorials in Metamaterials* (CRC, Boca Raton, 2011).
- [2] F. Capolino, *Theory and Phenomena of Metamaterials* (CRC, Boca Raton, 2009).
- [3] F. Capolino, *Applications of Metamaterials* (CRC, Boca Raton, 2009).
- [4] N. I. Zheludev, *Science* **328**, 582 (2010).
- [5] C. M. Soukoulis and M. Wegener, *Nat. Photonics* **5**(9), 523 (2011).
- [6] Q. Zhao, J. Zhou, F. Zhang, and D. Lippens, *Mater. Today* **12**, 60 (2009).
- [7] K. Vynck, D. Felbacq, E. Centeno, A. I. Căbuz, D. Cassagne, and B. Guizal, *Phys. Rev. Lett.* **102**, 133901 (2009).
- [8] Y. Kivshar, A. Miroshnichenko, A. Kuznetsov, and B. Lukyanchuk, Magnetic light and all-dielectric nanophotonics, in *Transparent Opt. Networks (ICTON)*, 2014 16th Int. Conf., 2014 (unpublished), p. Tu.A5.1.
- [9] I. Vendik, M. Odit, and D. Kozlov, *Radio Eng.* **18**(2), 111 (2009).
- [10] F. Zhang, L. Kang, Q. Zhao, J. Zhou, and D. Lippens, *New J. Phys.* **14**, 033031 (2012).
- [11] S. O'Brien and J. B. Pendry, *J. Phys.: Condens. Matter* **14**, 4035 (2002).
- [12] J. A. Schuller, R. Zia, T. Taubner, and M. L. Brongersma, *Phys. Rev. Lett.* **99**, 107401 (2007).
- [13] I. B. Vendik, O. G. Vendik, and M. S. Gashirova, *Tech. Phys. Lett.* **32**, 429 (2006).
- [14] I. Vendik, O. Vendik, I. Kolmakov, and M. Odit, *Opto-Electron. Rev.* **14**, 179 (2006).
- [15] J. Wang, Z. Xu, Z. Yu, X. Wei, Y. Yang, J. Wang, and S. Qu, *J. Appl. Phys.* **109**, 084918 (2011).
- [16] P. Moitra, Y. Yang, Z. Anderson, I. I. Kravchenko, D. P. Briggs, and J. Valentine, *Nat. Photonics* **7**, 791 (2013).
- [17] R. M. Bakker, D. Permyakov, Y. F. Yu, D. Markovich, R. Paniagua-Domínguez, L. Gonzaga, A. Samusev, Y. Kivshar, B. Luk'yanchuk, and A. I. Kuznetsov, *Nano Lett.* **15**, 2137 (2015).
- [18] L. Jelinek and R. Marqués, *J. Phys.: Condens. Matter* **22**, 025902 (2010).
- [19] M. I. Bakunov, A. V. Maslov, S. M. Kuznetsova, and S. N. Zhukov, *Phot. Nanostruct.: Fundam. Appl.* **12**, 114 (2014).
- [20] A. V. Maslov, S. M. Kuznetsova, M. Hangyo, and M. I. Bakunov, *J. Opt.* **16**, 125104 (2014).
- [21] R. Yahiaoui, H. Němec, P. Kužel, F. Kadlec, C. Kadlec, and P. Mounaix, *Appl. Phys. A* **103**, 689 (2011).
- [22] R. Yahiaoui, H. Němec, C. Kadlec, F. Kadlec, P. Kužel, U. C. Chung, C. Elissalde, M. Maglione, and P. Mounaix, *Appl. Phys. A* **109**, 891 (2012).
- [23] A. Andryieuski, S. Ha, A. A. Sukhorukov, Yu. S. Kivshar, and A. V. Lavrinenko, *Phys. Rev. B* **86**, 035127 (2012).
- [24] A. M. Nicolson and G. F. Ross, *IEEE Trans. Instrum. Meas.* **19**, 377 (1970).
- [25] D. R. Smith, S. Schultz, P. Markoš, and C. M. Soukoulis, *Phys. Rev. B* **65**, 195104 (2002).
- [26] C. R. Simovski, *J. Opt.* **13**, 013001 (2011).
- [27] C. R. Simovski, [arXiv:cond-mat/060622v1](https://arxiv.org/abs/cond-mat/060622v1).
- [28] C. R. Simovski and S. A. Tretyakov, *Phys. Rev. B* **75**, 195111 (2007).
- [29] C. R. Simovski, *Opt. Spectrosc.* **107**, 726 (2009).
- [30] T. Koschny, P. Markos, D. R. Smith, and C. M. Soukoulis, *Phys. Rev. E* **68**, 065602 (2003).
- [31] A. Andryieuski, C. Menzel, C. Rockstuhl, R. Malureanu, F. Lederer, and A. Lavrinenko, *Phys. Rev. B* **82**, 235107 (2010).
- [32] M. Albooyeh, D. Morits, and S. A. Tretyakov, *Phys. Rev. B* **85**, 205110 (2012).
- [33] S. A. Tretyakov, *Analytical Modelling in Applied Electromagnetics* (Artech House, Boston, 2003).
- [34] F. B. Arango and A. F. Koenderink, *New J. Phys.* **15**, 073023 (2013).
- [35] S. Lannebère, S. Campione, A. Aradian, M. Albani, and F. Capolino, *J. Opt. Soc. Am. B* **31**, 1078 (2014).
- [36] S. Campione, S. Lannebère, A. Aradian, M. Albani, and F. Capolino, *J. Opt. Soc. Am. B* **29**, 1697 (2012).
- [37] S. Campione, M. B. Sinclair, and F. Capolino, *Phot. Nanostruct.: Fundam. Appl.* **11**, 423 (2013).
- [38] S. Campione and F. Capolino, *Radio Sci.* **47**, RS0N06 (2012).
- [39] C. R. Simovski, S. Zouhdy, and V. V. Yatsenko, *Radio Sci.* **40**(5), RS5008 (2005).
- [40] U. Zywiets, A. B. Evlyukhin, C. Reinhardt, and B. N. Chichkov, *Nat. Commun.* **5**, 3402 (2014).
- [41] R. Paniagua-Domínguez, F. López-Tejeira, R. Marqués, and J. A. Sánchez-Gil, *New J. Phys.* **13**, 123017 (2011).
- [42] CST Computer Simulation Technology AG, <http://cst.com>.
- [43] B. Su, J. Holmes, C. Meggs, and T. Button, *J. Eur. Ceram. Soc.* **23**, 2699 (2003).